Available online at www.sciencedirect.com
ScienceDirect
Diamond & Related Materials 17 (2008) 931–936
DIAMOND AND RELATED MATERIALS
www.elsevier.com/locate/diamond

Graphite-to-diamond transformation induced by ultrasound cavitation

A.Kh. Khachatryan [a,c], S.G. Aloyan [a,*], P.W. May [b], R. Sargsyan [a], V.A. Khachatryan [a], V.S. Baghdasaryan [d]

[a] Institute of General and Inorganic Chemistry of Armenian National Academy of Sciences, 10 Argutyan 2 District, 0051, Yerevan, Armenia
[b] School of Chemistry, University of Bristol, Cantock's Close, Bristol BS8 ITS, U.K.
[c] Institute of Chemical Physics of Armenian National Academy of Sciences 5/2 Paruir Sevak St., 0044 Yerevan, Armenia
[d] Yerevan Physics Institute 2 Alikhanian Br. St., 0036 Yerevan, Armenia

Received 5 September 2007; received in revised form 14 January 2008; accepted 24 January 2008
Available online 13 February 2008

Abstract

Diamond microcrystals have been synthesized using ultrasonic cavitation of a suspension of hexagonal graphite in various organic liquid media, at an average bulk temperature of the liquid up to 120°C and at atmospheric pressure. The yield of diamond is up to 10% by mass. The diamonds were characterized by scanning electron microscopy, X-ray diffraction and laser Raman spectroscopy. Analysis of the crystallite size distribution showed that the diamonds were nearly mono-dispersed, having a size 6 or 9μm ± 0.5μm, with cubic, crystalline morphology.

Keywords: Ultrasound cavitation; Microcrystalline diamond

1. Introduction

Synthesis of diamond by a variety of chemical and physical routes is currently a topic of great scientific and commercial interest. Production of single crystal diamond particles of sizes between a few nm and several mm usually require process pressures in excess of tens of thousands of atmospheres and temperatures > 2000K in order to convert graphite into diamond. This is the basis of the so-called high pressure–high temperature (HPHT) method, which produces much of the world's supply of 'industrial diamond' used for commercial cutting and drilling applications.

An alternative strategy for generating these high temperatures and pressures was reported by Flynn in 1986 [1]. He suggested that ultrasonic cavitation processes, if sufficiently powerful, should produce the necessary combination of pressure and temperature to allow graphite-to-diamond transformation in metal melts. Cavitation is an efficient method to concentrate low density elastic wave energy into higher densities, as a result of the rapid collapse of cavitation bubbles produced in a suitable liquid medium [2]. The overall picture of cavitation bubble formation is as follows. As an elastic (sound) wave passes through a liquid, it produces alternating regions of reduced density (negative pressure) and increased density (positive pressure). If the sound wave is sufficiently intense, the reduced density regions form cavities (bubbles) filled with the saturated vapor of the liquid. Any gases dissolved in the fluid diffuse through the cavity walls and also contribute to the vapor inside the bubble.

In the contraction phase, the cavity collapses under the effect of positive pressure and surface tension forces, and the vapor-gas mixture within experiences a rapid, strong adiabatic compression. Depending upon the cavitation conditions, at the moment of collapse, the pressure, p, and temperature, T, inside the cavity may reach extremely high instantaneous values, $p \sim 10^5$–10^6bar, $T \sim 1000$K [3]. As a result of the simultaneous collapse of many cavities, a cavitation zone is formed in the ambient fluid. The cavitation zone can be considered to be a peculiar kind of "power transformer", in which energy is accumulated rather slowly (~ 10ms) during the negative pressure phase, but which is released on a very short timescale (~ 1ns). As a result, the

* Corresponding author.
E-mail address: samvelaloyan@yahoo.com (S.G. Aloyan).

0925-9635/$ - see front matter © 2008 Elsevier B.V. All rights reserved.
doi:10.1016/j.diamond.2008.01.112

instantaneous power is many orders of magnitude greater than that of the average power introduced to the cavitation medium. These extreme conditions create a specific physical and chemical medium for realization of many chemical reactions, such as for obtaining nanomaterials [4–6]. The instantaneous high pressure–high temperature conditions also provide the correct environment for the graphite-to-diamond transition.

In 1974, Galimov published a theoretical study concerning the possibility of synthesising diamonds using the cavitation phenomenon [7]. Using a prototype ultrasonic reactor, he and co-workers then corroborated the prediction by successfully synthesising nanodiamonds by cavitation destruction of bensole [8]. However, the approach (nucleation of diamond directly from cavitation of liquid hydrocarbons) and the apparatus were low power and very small scale. Although they proved the concept was feasible, the yield (and efficiency) for their process was too low for it to be a commercial possibility. The most significant work on the development of cavitation methods for nanodiamond synthesis is the US patent "Method and means for converting graphite to diamond" granted to Hugh G. Flynn in 1986 [1]. The author discussed practically all aspects of cavitation processes in the melts of easily fusible metals (Al, Ga, In, Sn). The device construction is presented, and the conditions for achieving maximal cavitation effect on solid (graphite)-fluid (metal melt) boundary are described. A scheme of maintenance of spherical symmetry for the cavitation pocket is proposed to achieve maximum cavitation impulse. Although the apparatus and various technological aspects of the synthesis process are discussed in detail, there is no subsequent description of the synthesis product. We must therefore conclude that Flynn never successfully synthesised diamond by this route.

Other attempts at diamond synthesis by cavitation include Leonov et al. [9], who reported ultrasonic cavitation within hexane and ethanol, although the nanoparticles they produced were not characterized and may have been graphitic. Wang et al. [10] and Pearce et al. [11] energized cavitation by pulsed laser ablation (PLA) on solid (graphite) at a fluid (water, cyclohexane) boundary. However, diamond synthesis under PLA conditions is not energy efficient, and only nanosized diamond particles with low yield were reported using this method. For nanodiamond synthesis, generation of a high power cavitation impulse is not necessary. Therefore, it is possible to use practically any cavitation media, from organic (high- and low-boiling) to inorganic fluids (H_2O) [11]. For production of larger diamond crystallites (μm or even mm in size) cavitation effects in the presence of a solid carbon phase, such as a graphite target or suspended graphite particles may be the way forward.

During the last ten years, theoretical and experimental research into the growth dynamics and collapse of cavitation bubbles has achieved pressures ($p \sim 10^{10}$–10^{12}bar) and temperatures ($T \sim$ 7000K), sufficient for thermonuclear reaction in deuterium/acetone [12–15]. Authors of these works have applied a new approach to vapour cavitation in order to overcome the problem of the cavitation bubbles losing their spherical symmetry during collapse — previously a major constraining factor for the maximum temperatures and pressures attainable. The process of cavitation bubble collapse was studied by Nigmatulin et al. [15,16]. Their calculations were based on the HYDRO program developed by Moss et al. [17] with a series of additions, which allowed the theory to be extended to higher temperatures and pressures. The description of the bubble collapse was based on numerical solution of a set of equations in the form of mass, energy and impulse conservation laws for gaseous and fluid phases, assuming spherical symmetry of the collapsing cavity, and taking into account the medium velocity, pressure and temperature. They included also the Hertz–Knudssen–Lengmure conditions on the phase boundary, taking into account the fluid condensing coefficient, α.

The results of these investigations highlighted the importance of the cavity medium properties for the formation of super-high pressure shockwaves when the cavities collapse, and determined the cavitation fluid parameters at which the spherical shape of the bubbles is maintained up to the final stage of collapsing. These include that the cavitation medium should be a well degassed (organic) fluid composed of large molecules, with a low vapour pressure, and have a low vapour-phase acoustic velocity, a high condensation coefficient ($\alpha \sim 1$) and high cavitation strength.

For the right choice of medium, cavitation could be an ideal method for generation of a high-power cavitation impulse. In these conditions, the temperature drop behind the pressure-shockfront occurs extremely rapidly, $\sim 10^{10}$K s^{-1} [18]. Hence, in cavitation processes, ultra-high energies are possible for time-scales of a few ns, which can act locally upon the substances in the region of the collapsing cavities resulting in shock compressions. Within these compressions, strongly developed density fluctuations allow rapid and reversible clustering of substances, where the state of the substance (solid, liquid or vapour) can vary rapidly [18,19,]. This is exactly what is required for the extreme compression of graphite needed for diamond synthesis [20,21].

The purpose of this investigation is to demonstrate the feasibility of using such high power cavitation processes to produce microsized synthetic diamond particles.

2. Experimental

Fig. 1 shows the cavitation module designed for microdiamond synthesis. The module consists of a reactor (1), composed

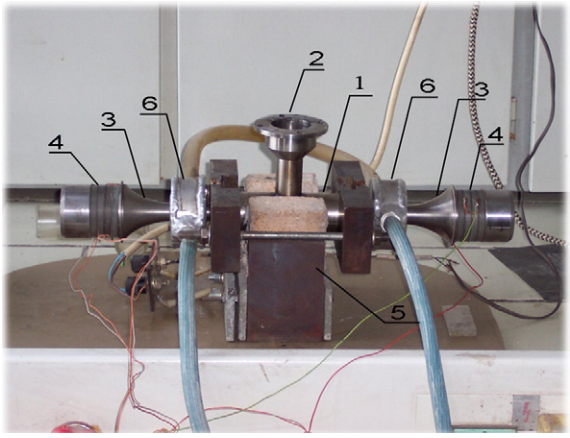

Fig. 1. The experimental cavitation module used in this study.

of a 100mm-long tube made from stainless steel or heat-resistant glass with inner diameter of 25mm. The central portion of the reactor has a charging hole (2), from which to input or extract the liquid media. Two ultrasonic emitters (3), attached to a package of titanium concentrators with ZTBS-3 piezoceramic discs (4), are fixed to opposite ends of the reactor. The radiating surface diameter is 20mm for each concentrator. The reactor (1) is water cooled and controlled by a thermostabilization feedback system (5). If required, the emitters can be cooled by radiators (6).

A 23kHz sine-wave generator with output power of 1000W and self-tuning resonance frequency was used to initiate cavitation. The maximum ultrasound intensity in the reactor centre was 75–80W cm^{-2} (corresponding to a sound pressure amplitude of about 15–16bar). The ultrasound intensity was determined according to the Margulis–Maltsev procedure [22].

Experiments were carried out in two modes: at maximum ultrasound intensity (series 1) and at 80% of the maximum level (series 2). Each series consisted of four experiments. As cavitation fluids, a series of aromatic oligomers of formula $C_nH_mO_x$ (n = 18–36; m = 14–26; x = 2–5) were synthesized. This oligomeric series was chosen for its low saturated vapour pressure and rather high boiling temperatures. Also, some compounds from this series are used as the stationary phase in gas chromatography, and therefore information about their condensing coefficients at the fluid-gas boundary ($\alpha \sim 1$) is known [23]. For the selected compound (an isomeric mixture of five- and six-ring polyphenyl ethers, with the mass fraction of the six-ring polyphenyl ethers equal to 11%), a suspension was made with powdered (100–200μm) special purity graphite. The total amount of inorganic impurities present in the graphite was $\sim 3 \times 10^{-3}$ mass%, see Table 1. The solid–fluid weight ratio for the suspension was 1:6 in all experiments, and the cavitation fluid density was 1.1g cm^{-3} at 25°C. The reactor was filled (52ml) with the suspension via the charging hole.

Prior to synthesis, the suspension was degassed by pumping the system through the charging hole using a vacuum pump to a base pressure of 20mTorr while simultaneously initiating the ultrasound at 20% of maximum power for ~ 10min. During this degassing process, an intensive release of gas bubbles was observed, and the reaction mixture increased in temperature to 80–100°C.

Diamond synthesis was started with the reaction mixture temperature at 80°C by smoothly increasing the ultrasonic power up to its maximum value. This power increase was accompanied by the formation of cavitation zones over the whole reactor volume, accompanied by a characteristic crackling sound. The synthesis process was terminated when the reaction mixture temperature reached 120°C, typically after 2min for the given reactor cooling mode. Some experiments were carried out for longer times (up to 12min). Note that the temperature quoted above is that of the bulk reaction mixture; the local reaction temperature will, of course, be much higher, of the order of many thousands of K. Ideally, we would like to characterize the growth conditions by measuring the local temperature, pressure and size of the cavitation bubbles. These experiments are currently underway and the results will be presented in a subsequent publication.

Table 1
Most abundant inorganic impurities (units of % by mass) present in the initial graphite and in the diamond product, as measured by an emission spectral analyzer DFS-13

Impurity	Initial graphite	Diamond
Al	1.8×10^{-4}	1.7×10^{-4}
Fe	5.5×10^{-4}	5.6×10^{-4}
Si	3.1×10^{-3}	3.0×10^{-3}
K	7.0×10^{-4}	5.0×10^{-3}
Mg	7.7×10^{-4}	7.5×10^{-4}
P	3.1×10^{-4}	3.0×10^{-4}
Cr	1.0×10^{-5}	1.0×10^{-4}

After each experiment, the liquid phase was allowed to cool, then removed from the reactor. It was then separated from the solid synthesis product by centrifuging. The solid phase was washed using acetone, then a control sample was collected, and the remainder was oxidized using sulfochromic mixture (H_2SO_4 + $K_2Cr_2O_7$ acids [24]) to remove any non-diamond carbon phase. The diamond yield was determined by weighing the solid before and after oxidation. Losses of the diamond phase during separation did not exceed 5%. To accumulate sufficient synthesis product for further analysis, samples from four identical experiments in each series were mixed together.

The solid-state products of synthesis were examined using X-ray analysis (URD-6 X-ray diffractometer $K_{Cu-\alpha}$ with wavelength 1.544Å), scanning electron microscopy, SEM (JEOL 2010 for series 1, REM-100Y for series 2), and laser Raman spectroscopy (Renishaw 2000 Raman Spectrometer). The content of micro-impurities was determined by an emission spectral analyzer DFS-13. The size distribution of the synthesized diamonds was determined by software (ImageJ v.1.38) analysis of SEM images of these diamonds.

3. Results and discussion

In all ultrasound experiments using the graphite powder suspension, we observed formation of a solid product that was not oxidisable by sulfochromic mixture. X-ray analysis of this non-oxidisable product (Fig. 2) produced peaks corresponding to d-spacings of d = 2.058Å and 1.262Å, 1.0752Å, which are consistent with literature values for the cubic diamond unit cell (e.g. 2.06Å, 1.26Å and 1.075Å for the {111}, {220} and {311} planes, respectively [25]). Also shown in Fig. 2 is the X-ray pattern from the initial graphite, for comparison.

During the 2min cavitation, the yield of diamond in all experiments was ~ 0.5% of the initial graphite mass for series 1, and ~ 2% for series 2. Fig. 3 shows SEM images of the synthesized diamond particles. Photomicrography analysis reveals that each particle is a shaped microcrystal with distinguishable growth faces. The particle form factor was 1.1 to 1.2. Fig. 4 presents a distribution bar chart of the diamond particle sizes for both series. For all experiments, nearly monodispersed diamond powder was obtained, with series 1 producing 6μm crystallites and series 2 producing 9.5μm crystallites, with a size spread in both cases of ~ 0.5μm. This spread may simply be a result of mixing the diamond products from 4 experiments, where weak fluctuations of electrical

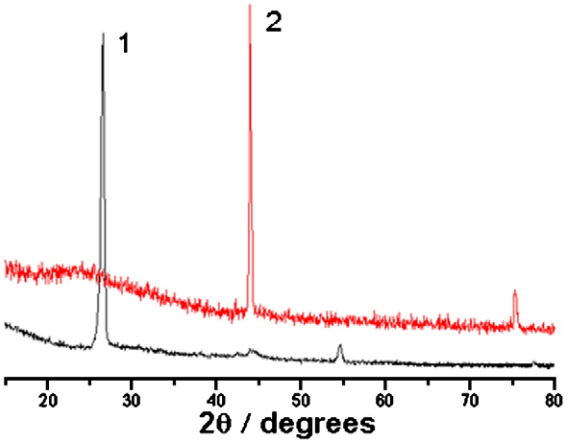

Fig. 2. X-ray patterns of (1) the initial graphite and (2) the solid, non-oxidisable product after cavitation. The peaks in (2) at $2\theta = 44°$ and $2\theta = 76°$ correspond closely to those expected for diamond peaks with *d*-spacings 2.06 Å (111 plane) and 1.26 Å (220 plane), respectively [25].

parameters were inevitable. Alternatively, the spread may be a result of inaccuracies in the software analysis.

Of particular interest is the correlation between particle sizes in each series with the diamond phase yield. Mathematical processing of the diamond phase yield data and the particle size (in view of equal particle size in each series) in series 1 and 2 allows us to calculate that, in each experiment, an equal amount of diamond particles is formed.

An apparent conclusion from these experimental results is that the diamond formation process is of probabilistic nature, i.e. that it is controlled by the number of "successful" (resulting in the diamond phase formation) cavity collapses. We believe these occur when the shockwave is directed normally to the randomly-oriented graphite basal planes. Each particle of the graphite (sized 100–200μm) is a sintered agglomerate consisting of randomly oriented crystallites. We believe that each "successful" collapse is a cavitation implosion directed normally to the basal planes of separate individual crystallites. Since there are many crystallites oriented along different directions, there is a high probability that any given cavitation collapse will be normal to at least one of these crystallites, resulting in high yield. To confirm this, an experiment was performed under identical conditions but using quasi-monocrystalline graphite (particle size ~ 100–200μm) having highly oriented basal planes. For these, the probability of a cavitation collapse being normal to the graphite particle surface is much lower, since on average the crystals will be oriented in the wrong direction far more often than in the normal direction. As expected, the cavitation experiment now formed diamond only in trace quantities, insufficient for analytical examination. This suggests that the graphite-to-diamond transformation results from the collapse of a single cavitation bubble that formed on the graphite surface (one "successful" collapse = one diamond crystal).

The form of the particle size distribution curve is related to their formation mechanism [26]. The very narrow spread of particle sizes (± 0.5μm) observed in both growth series suggests that the synthesis is terminated rapidly after the shock wave has passed. This is because the formation of monodispersed diamond crystallites sized up to 10μm in such short time periods cannot be explained by the existing models of diamond

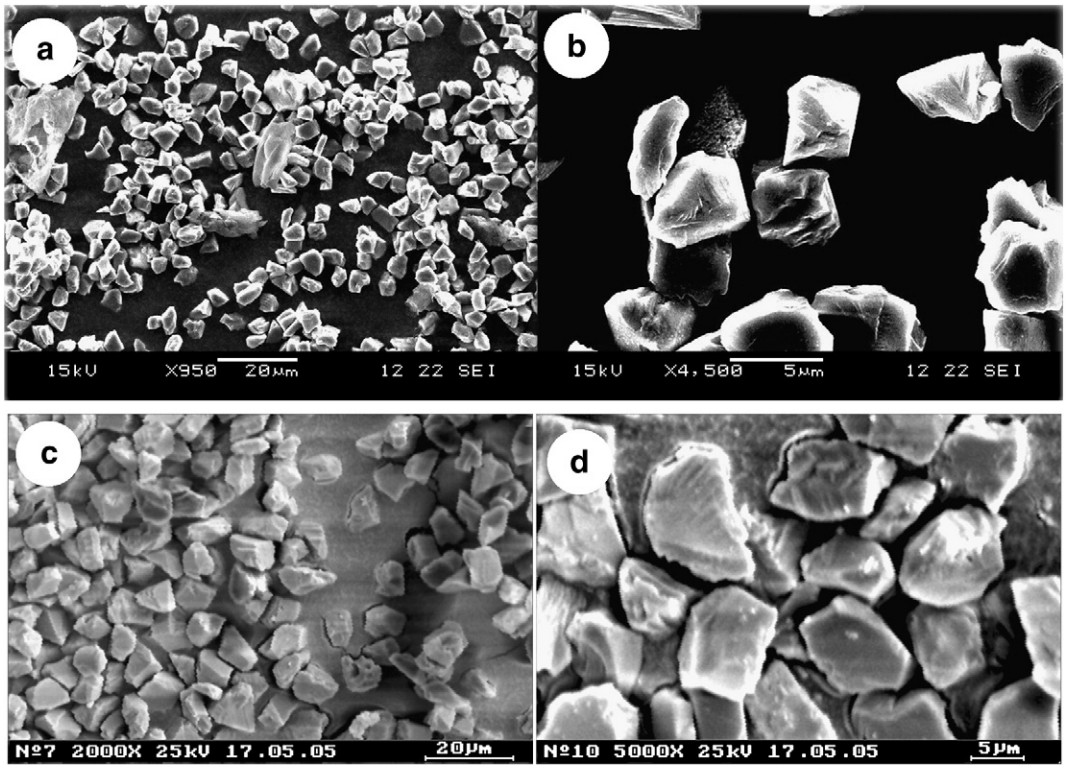

Fig. 3. SEM images of the cavitation diamonds: (a), (b) series 1 (taken at Bristol); (c), (d) series 2 (taken at Yerevan).

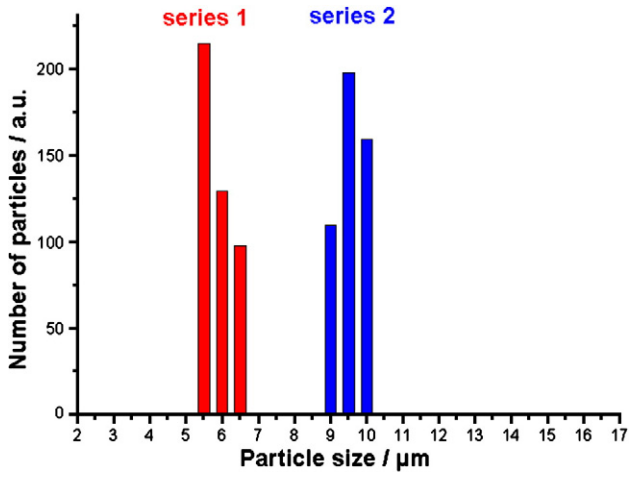

Fig. 4. Size distribution bar chart for diamond particles from both series. Both series contained a mixture of the products of four identical experiments.

cluster growth [27]. At extreme conditions diamond formation must occur by another mechanism.

Table 1 presents data on the impurity composition for seven elements contained in both the initial graphite and the synthesized diamonds. Analysis shows that the impurity concentrations of the synthesized diamond are almost identical to those of the initial graphite (although an increased content of potassium and chromium in the diamond is related to the acid treatment during product separation).

Fig. 5 presents Raman spectra of (a) the initial graphite, (b) the unpurified graphite/diamond product following cavitation, and (c) the separated diamonds, for series 2, using green (514 nm) laser excitation. For the starting material, as expected, the Raman spectrum shows only the 1580 cm^{-1} and (small) 1380 cm^{-1} peaks characteristic of ordered and disordered graphite, respectively. For the unpurified cavitation product, both the 1580 cm^{-1} peak and the 1332 cm^{-1} peak (characteristic of crystalline diamond) appear. For the purified diamond product only the 1332 cm^{-1} peak is present. This shows that the purification process was successful in removing virtually all the sp^2 carbon material from the product, leaving pure diamond. The rising photoluminescent background is typical of small-grained diamond and results from defects in the crystallites and scattering from crystal edges. It is also worth mentioning that the Raman spectra were easily capable of detecting the presence of the diamond phase within the cavitation product at a concentration of 1.5%. This suggests that Raman analysis might prove an invaluable tool for process optimization and control when developing this synthesis method further.

As well as initiating diamond formation, the cavitation process 'crushes' the graphite into smaller particles, which appear to be less efficient at making diamond. To investigate this, experiments were performed using various sizes of graphite (0–50, 50–63, 100–150, 100–200, and 100–250 μm). Diamonds were only obtained for the largest three sizes. After the synthesis the solid phase was separated out, dried and sieved (100 μm hole size) to determine what fraction of the graphite had been crushed into smaller particles. After a synthesis time of 2 min, we found that ~5% of the graphite (initial size 100–200 μm) had been crushed, and passed through the 100 μm sieve. This 5% was oxidized separately, but after analysis found to contain no diamonds. Diamonds were found, however, after oxidizing the larger graphitic fraction (that did not pass through the sieve). This suggests that diamond formation requires large (>60 μm) graphitic particles, and that the diamond may have formed inside or at the surface of these particles. However, SEM analysis of the graphite after the synthesis was inconclusive, and the question remains open. One possible explanation for the size effect is that the kinetic energy of the shockwave is not absorbed by small mass graphitic particles, and 'by-passes' them, whereas the more massive particles, with their higher inertia, experience the full shock wave.

A consequence of this, however, is that continuation of the cavitation process beyond a few minutes is unfortunately *not* accompanied by an increase in the diamond yield. This is because as cavitation proceeds, the graphite particle size reduces and the efficiency of diamond production drops. However, manifold increases in yield can be achieved by completely refilling the cavitation medium while maintaining the solid phase. The maximum yield of microdiamonds for the 10 μm fraction was 10 mass% after 6 complete refillings of the cavitation fluid. Hence, the limiting stage of cavitation synthesis is the change of the cavitation medium chemical composition. Note that the cavitation medium is easily regenerable by pumping down, and that it can be used repeatedly.

Unfortunately, it is not yet possible to specify an optimum composition (initial or intermediate) of the cavitation media for reaching the maximum cavitation impulse, and therefore for diamond formation. It is also possible that easily volatile and gaseous products from the destruction of the cavitation medium may result in a premature elastic collapse of the cavities and attenuate the cavity impulse.

It is worth comparing the energy efficiency of this cavitation process with other methods of making diamond. Our ultrasonic reactor delivers 1 kW for a total reaction time of ~2 mins, which translates into a total energy delivered to the reaction chamber of 120 kJ. Since ~10 g of graphite was initially present in the reactor and (for the 9.5 μm fraction) 2% of this was

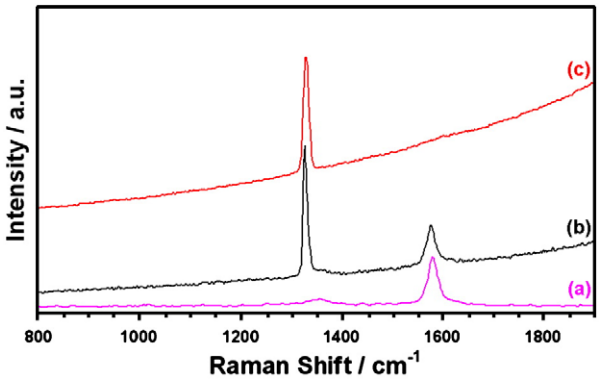

Fig. 5. Laser Raman spectrum (514 nm) of (a) the graphite starting material, (b) the unpurified product containing ~1.5% diamond in graphite, and (c) the purified (100%) diamond product. The spectra have been offset vertically for clarity.

converted to diamond, the total yield was ~0.2 g of diamond (1 carat). Therefore the cavitation process requires 600 kJ per gram of diamond. Compare this to a typical 1 kW microwave CVD reactor, which grows, say, 5 μm of diamond over an area of 1 cm^2 in an hour. This would have an energy usage of 2000 MJ g^{-1} of diamond. Similarly, for HPHT diamond, the efficiency is estimated to be ~400 kJ g^{-1} of diamond. This shows that ultrasonic cavitation is a very energy efficient route to forming diamond compared to CVD, and comparable to that for HPHT. If developed successfully, this technology, therefore, has the potential to be a realistic commercial prospect.

4. Conclusions

We have shown that, although at an early stage of development, the cavitation synthesis method opens new opportunities in obtaining diamond crystallites at relatively benign conditions, average bulk temperature of the liquid up to 120 °C and at atmospheric pressure. It produces crystalline diamonds with a very sharp, well defined size range of 5–10 μm, and with high purity. The major factor influencing diamond yield in the cavitation process is the composition of the cavitation medium, and there is wide scope here for future experiments. Furthermore, the rapid timescale for diamond formation may allow controllable doping with selected impurities such as N or B, with a view to obtain p- and n-type semiconducting diamonds. An optimum method of cavitation generation (pulse or periodic signal) may enable us to maintain a constant composition of cavitation medium and, consequently, to increase the diamond yield considerably. The absolute size of the synthesized diamond powders and their size distribution are related to the synthesis conditions (p and T). Hence, it is possible to determine quantitative energy characterization of cavitation perturbations.

Our present cavitation module allows up to 10% graphite-to-diamond conversion in a continuous regime of regeneration for the cavitation medium, thus opening commercial prospects for the method. Future designs could increase this yield further. With suitable choice of cavitation media, the cavitation method could be used for synthesis of other potentially important compounds, such as cubic boron nitride, carbon nitride, etc.

Acknowledgments

The authors are grateful to all who rendered technical, material and moral support during the research. Special gratitude should be expressed to Dr V. Khachatryan, a specialist in organic synthesis, for the help in the cavitation media synthesis, and to Prof. N. Ananikyan, a specialist in theoretical physics, for useful advices on the process mechanism.

References

[1] H.G. Flynn, United States Patent 4,563,341, January 7, 1986.
[2] H.G. Flynn, Physics of acoustic cavitation in liquids, in: W.P. Mason (Ed.), PhysicalAcoustics, vol. 1B, Academic Press, New York, 1964, p. 7.
[3] C.E. Brennen, Cavitation and Bubble Dynamics, Oxford University Press, Oxford, 1995.
[4] A. Khachatryan, R. Sargsyan, L. Hasratyan, V. Khachatryan, Ultrason. Sonochem. 11 (2004) 405.
[5] J.-L. Delplancke, J. Dille, J. Reisse, G.J. Long, A. Mohan, F. Grandjean, Chem. Mater. 12 (2000) 946.
[6] K.S. Suslick, M. Fang, T. Hyeon, J. Am. Chem. Soc. 118 (1996) 11960.
[7] E.M. Galimov, Nature 243 (1973) 389.
[8] E.M. Galimov, A.M. Kudin, V.N. Skorobogatski, V.G. Plotnichenko, O.L. Bondarev, B.G. Zarubin, V.V. Strazdovski, A.S. Aronin, A.V. Fisenko, I.V. Bykov, A. Yu. Barinov, Dokl. Phys. 49 (2004) 150.
[9] G.V. Leonov, A.L. Vereschagin, O.V. Lavrinenko, International Workshops and Tutorials on Electron Devices and Materials EDM 2006: Workshop Proceedings, NSTU, Novosibirsk, 2006.
[10] G.W. Yang, J.B. Wang, Appl. Phys., A Mater. Sci. Process. 72 (2001) 475.
[11] S.R.J. Pearce, S.J. Henley, F. Claeyssens, P.W. May, K.R. Hallam, J.A. Smith, K.N. Rosser, Diamond Relat. Mater. 13 (2004) 661.
[12] R.I. Nigmatulin, I.Sh. Akhatov, A.S. Topolnikov, N.K. Vakhitova, R.T. Lahey, R.P. Taleyarkhan, Phys. Fluids 17 (2005) 107106.
[13] R.P. Taleyarkhan, C.D. West, J.S. Cho, R.T. Lahey Jr., R.I. Nigmatulin, R.C. Block, Science 295 (2002) 1868.
[14] R.P. Taleyarkhan, J.S. Cho, C.D. West, R.T. Lahey Jr., R.I. Nigmatulin, R.C. Block, Phys. Rev., E 69 (2004) 036109.
[15] R. Nigmatulin, Nucl. Eng. Des. 235 (2005) 1079.
[16] R.I. Nigmatulin, R.P. Taleyarkhan, R.T. Lahey, J. Power Energy 128 (2004) 345.
[17] W.C. Moss, D.B. Clarke, J.W. White, D.A. Young, Phys. Lett., A 211 (1996) 69Phys. Fluids 6 (1996) 2979.
[18] E.N. Avrorin, B.K. Vodolaga, V.A. Simonenko, V.E. Fortov, Successes Phys. Sci. 163 (1993) 1.
[19] Y.B. Zeldovich, Y.P. Raizer, Physics of Shock Waves and High-Temperature Hydrodynamic Phenomena, Academic Press, New York, 1966.
[20] R.K. Belheeva, Siberian J. Ind. Math. 10 (2007) 25.
[21] R.K. Belheeva, Proc. physics of extreme conditions of substances conference, Chernogolovka, 2006, p. 117.
[22] M.A. Margulis, A.N. Maltsev, Russ. J. Phys. Chem. 43 (1969) 592.
[23] P. Clausing, Ann. Phys. 12 (1932) 961.
[24] A.A. Putjanin, I.V. Nikolskaya, A.J. Kalashnikov, Superhard Mater. 2 (1982) 20.
[25] Y. Gogotsi, S. Welz, D.A. Ersoy, M.J. McNallan, Nature 411 (2001) 284.
[26] U.I. Petrow, Clusters and Small Particles, Nauka, Moscow, 1986.
[27] E. Lin, Solid State Phys. 42 (2000) 1893.